THE ASTROPHYSICAL JOURNAL, 454:420–428, 1995 November 20

RADIATIVE $He^+(1s) + He(1s^2)$ PROCESSES AS THE SOURCE OF THE DB WHITE DWARF ATMOSPHERE ELECTROMAGNETIC CONTINUOUS SPECTRA

A. A. MIHAJLOV,[1,2] M. S. DIMITRIJEVIĆ,[2] LJ. M. IGNJATOVIĆ,[1] AND Z. DJURIĆ[1]
Received 1994 August 12; accepted 1995 May 1

ABSTRACT

The influence of the processes of radiative charge transfer and photoassociation during $He^+ + He$ collisional processes, as well as the process of the photodissociation of the He_2^+ molecular ion, on the formation of the continuous spectrum of the DB white dwarf atmospheres with $T_{eff} = 12{,}000$–$30{,}000$ K, for log g (gravity) = 7 and 8, is studied within the wavelength range $\lambda = 200$–800 nm. It is shown that the contribution of these processes relative to other relevant radiative processes is particularly important for $T_{eff} \leq 16{,}000$ K and increases with the decrease of T_{eff}. Moreover, it is found that the influence of the considered $He^+ + He$ radiative processes is particularly pronounced in the UV range.

Subject headings: atomic processes — radiative transfer — stars: atmospheres — white dwarfs

1. INTRODUCTION

Radiative $He^+(1s) + He(1s^2)$ processes may be of importance for the formation of continuous spectra in helium-rich star low-temperature atmospheric layers (see, e.g., Mihajlov & Dimitrijević 1992; Stancil 1994). In this work, such radiative processes within DB white dwarf atmospheres are investigated in detail. Special attention is paid to their contribution to the formation of continuous optical spectra, as a function of the effective temperature T_{eff} and log g (gravity), in comparison with the contribution of other relevant radiative processes. Here we will consider the ion-atom processes of photoassociation and photodissociation

$$He^+(1s) + He(1s^2) \Leftrightarrow \epsilon_\lambda + He_2^+ , \qquad (1a)$$

as well as the processes of the photoemission and photoabsorption charge exchange

$$He^+(1s) + He(1s^2) \Leftrightarrow \epsilon_\lambda + \begin{cases} He^+(1s) + He(1s^2) \\ He(1s^2) + He^+(1s) \end{cases} , \qquad (1b)$$

where $He_2^+ = He_2^+(1\Sigma_u^+)$ and ϵ_λ is the energy of the photon with the wavelength λ. These processes will be considered here within the semiclassical approach (Mihajlov & Popović 1981; Mihajlov & Dimitrijević 1986, 1992). We will compare the influence of the ion-atom processes in equations (1a)–(1b) on the optical characteristics of the DB white dwarf atmospheres with the influence of other radiative processes which are also significant for these atmospheres. These include the processes of emission and absorption connected with the free-free transitions of an electron in the filed of atoms and atomic ions, as well as the processes of electron-ion photorecombination and photoionization of excited atoms. We take into account atoms and ions relevant for the assumed DB white dwarf atmosphere plasma composition (Bues 1970; Koester 1980). The contribution of the electron-atom processes will be estimated here in the manner of Bell, Berrington, & Croskery (1982), and the contribution of the electron-ion processes using the results of Sobelman (1979) and Menzel (1962).

The radiative processes investigated are considered within the optical range 200 nm $< \lambda <$ 800 nm. The needed calculations are performed for 12,000 K $\leq T_{eff} \leq$ 30,000 K and log g = 7 and 8. In such a way, the entire range of T_{eff} and log g parameters, considered in Koester (1980) concerning the white dwarf atmosphere modeling, is covered.

Our objective here is to estimate the importance of the ion-atom processes of photoassociation and photodissociation in equation (1a) and photoemission and photoabsorption charge exchange in equation (1b) in comparison with the relevant electron-atom and electron-ion processes in order to clarify the nature of the DB white dwarf photosphere continuous spectrum for different λ and T ranges. Therefore, we will study the influence of these processes on particular photospheric layers as well as their global characteristics. Such results may be of significance for DB white dwarf photosphere modeling.

The absorption channels (right to left implications) for the ion-atom reactions in equations (1a) and (1b) have been considered previously in Mihajlov & Dimitrijević (1992) and Stancil (1994). The contribution of emission channels (left to right implications) has been considered in Mihajlov, Ermolaev, & Dimitrijević (1993) for laboratory plasma and in Mihajlov, Dimitrijević, & Ignjatović (1994a) for a special case of DB white dwarf atmospheres.

2. THEORY

2.1. *Radiative Process Characteristics*

The contribution to the continuous spectra of the emission and absorption channels for ion-atom reactions in equations (1a) and (1b) can be characterized with the help of the corresponding partial spectral emissivities $\epsilon^{(a)}$ and $\epsilon^{(b)}$, the total emissivities $\epsilon^{(ab)} = \epsilon^{(a)} + \epsilon^{(b)}$, and the spectral absorption coefficients $\kappa^{(a)}$, $\kappa^{(b)}$, and $\kappa^{(ab)} = \kappa^{(a)} + \kappa^{(b)}$, respectively, where superscripts a and b denote the corresponding reactions. We will also use here the emissivity ϵ_{ea} and the absorption coefficient κ_{ea}, characterizing electron-atom radiative processes, and similarly ϵ_{ei} and κ_{ei}, characterizing electron-ion processes, as the source of the background opacity. All quantitities should be treated as functions of the wavelength (λ), temperature (T), and corresponding particle densities.

As a measure of the influence of the ion-atomic processes in equations (1a)–(1b) on the continuous spectra of white dwarf

[1] Institute of Physics, P.O. Box 57, 11001 Beograd, Yugoslavia.
[2] Astronomical Observatory, Volgina 7, 11050 Beograd, Yugoslavia.

atmospheres, we will use the quantity

$$F = \frac{\epsilon^{(ab)}}{\epsilon}, \quad (2)$$

where $\epsilon = \epsilon_{ea} + \epsilon_{ei}$. Besides this quantity, the ratio $\kappa^{(ab)}/\kappa$, with $\kappa = \kappa_{ea} + \kappa_{ei}$, may be used in principle as well. When LTE exists, then $\epsilon^{(ab)}/\epsilon = \kappa^{(ab)}/\kappa$. Outside LTE, however, these ratios are not equal, and one of them must be chosen. We consider here mainly outer atmospheric layers where the optical depth is less than or equal to unity. The radiation from such layers goes out, resulting in a departure from LTE by the excited atom population. For outer solar atmospheric layers, e.g., where a similar situation exists, this is confirmed by the direct plasma composition calculations (Vernazza, Avrett, & Loeser 1981). For DB white dwarfs, one may expect a similar situation. In the case of departure from LTE, the calculation of the absorption coefficient, κ, requires more information about excited atom populations. Consequently, we will take here the quantity F just given in equation (2) as in our previous work (see, e.g., Mihajlov et al. 1994a, b).

We will express $\epsilon^{(ab)}$ and $\kappa^{(ab)}$ in the form

$$\epsilon^{(ab)} = S^{(ab)} N(He^+) N(He), \quad \kappa^{(ab)} = K^{(ab)} N(He^+) N(He), \quad (3)$$

where $N(He^+)$ and $N(He)$ are densities of the helium ion and atom and $S^{(ab)}$ and $K^{(ab)}$ are the corresponding spectral coefficients for spontaneous emission and absorption, describing the ion-atom radiative processes in equations (1a) and (1b) together.

2.2. *Spectral Coefficients of Spontaneous Emission and Absorption*

Spectral coefficients $S^{(ab)}$ and $K^{(ab)}$ may be determined within the semiclassical approximation (Mihajlov & Popović 1981; Mihajlov & Dimitrijević 1992) and can be represented as functions of λ and temperature T in the form

$$S^{(ab)}(\lambda, T) = 4.777 \times 10^{-34} \frac{C(R_\lambda)}{1.345[1 - 0.362(a_0/R_\lambda)]} \times \left(\frac{R_\lambda}{a_0}\right)^4 \left(\frac{\epsilon_\lambda}{2Ry}\right)^5 \exp\left[\frac{-U_2(R_\lambda)}{kT}\right], \quad (4)$$

$$K^{(ab)}(\lambda, T) = 0.620 \times 10^{-42} \frac{C(R_\lambda)}{1.345[1 - 0.362(a_0/R_\lambda)]} \times \left(\frac{R_\lambda}{a_0}\right)^4 \theta(\lambda, T) \exp\left[\frac{-U_1(R_\lambda)}{kT}\right], \quad (5)$$

where the coefficient $C(R_\lambda)$ is given by

$$C(R_\lambda) = \left[\frac{2D_{12}(R_\lambda)}{eR_\lambda}\right]^2 \frac{1.345[1 - 0.362(a_0/R_\lambda)]}{\gamma(R_\lambda)},$$

$$\gamma(R_\lambda) = \left|\frac{d \ln \{[U_2(R) - U_1(R)]/2Ry\}}{d(R/a_0)}\right|_{R=R_\lambda}. \quad (6)$$

Here R denotes the internuclear distance in the $He^+ + He$ system; $U_1(R)$ and $U_2(R)$ are adiabatic terms of the ground ($1\,\Sigma_u$) and the first excited electronic states ($1\,\Sigma_g$) of the He_2^+ ion, which are given in Gupta & Madsen (1967); and R_λ denotes the R value such that

$$U_2(R_\lambda) - U_1(R_\lambda) = \epsilon_\lambda, \quad (7)$$

where $\epsilon_\lambda = 2\pi\hbar c/\lambda$, and $D_{12}(R)$ is the module of the dipole matrix element taken between these two states. In our previous work, the approximation $D_{12}(R) = eR/2$ was used. Here we use the following expression (Ermolaev & Mihajlov 1991), more accurate in the visible spectral range:

$$D_{12}(R) = \frac{eR}{2} \frac{1 - 0.695(a_0/R)}{(1 - s^2)^{1/2}},$$

$$s = \left[1 + 1.345\frac{R}{a_0} + \frac{1}{3}\left(1.345\frac{R}{a_0}\right)^2\right] \exp\left(-1.345\frac{R}{a_0}\right), \quad (8)$$

where s denotes the integral of the He $1s$ orbital overlapping for a given R. Finally, the coefficient $\theta(\lambda, T)$, which describes the decrease of the absorption coefficient resulting from stimulated emission, is given by the expression

$$\theta(\lambda, T) = 1 - \exp\left(-\frac{\epsilon_\lambda}{kT}\right). \quad (9)$$

From equations (4), (5), (7), and (9), it follows that the ratio $S^{(ab)}/K^{(ab)}$ represents the universal function of λ and T (see, e.g., Sobelman 1979), proportional to the Planck distribution function. One must take into account that numerical coefficients in equations (4) and (5) are chosen in such a manner that $S^{(ab)}$ is expressed in J cm^{-3} s^{-1} nm^{-1} and $K^{(ab)}$ is expressed in cm^5. All parameters needed for the calculation of spectral coefficients $S^{(ab)}$ and $K^{(ab)}$ in the 150 nm $\leq \lambda \leq$ 850 nm range are given in Table 1. The behavior of these coefficients as a function of T is presented in Figures 1 and 2.

Stancil (1992, his Figs. 4–5) compares his results for the absorption coefficient with the corresponding semiclassical results for H (Mihajlov & Dimitrijević 1986) and He (Mijajlov & Dimitrijević 1992). He found good agreement between quantum-mechanical and semiclassical results for He, better than for H. This is the consequence of the fact that in Mihajlov & Dimitrijević (1986), the approximate expressions for molecular terms and $\gamma(R_\lambda)$ factor (not used in Mihajlov & Dimitrijević 1992 for helium) have been used. Moreover, in comparison with Mihajlov & Dimitrijević (1992), the expressions given here are more accurate for the dipole matrix elements. In Stancil (1994), the photodissociation channel contribution has been considered using the quantum-mechanical approach, while the

TABLE 1

PARAMETERS NEEDED FOR CALCULATION OF SPECTRAL COEFFICIENTS[a]

λ (nm)	R_λ (a.u.)	ϵ_λ (a.u.)	$\lvert U_1(R_\lambda)\rvert$ (a.u.)	$U_2(R_\lambda)$ (a.u.)	$C(R_\lambda)$
150.....	2.20	0.3037	0.0832	0.2205	1.052
200.....	2.43	0.2278	0.0755	0.1523	1.037
250.....	2.62	0.1822	0.0672	0.1150	1.029
300.....	2.77	0.1519	0.0600	0.0918	1.025
350.....	2.90	0.1302	0.0540	0.0761	1.022
400.....	3.01	0.1139	0.0490	0.0649	1.020
450.....	3.11	0.1012	0.0448	0.0564	1.019
500.....	3.19	0.0911	0.0412	0.0499	1.018
550.....	3.27	0.0828	0.0382	0.0446	1.017
600.....	3.35	0.0759	0.0356	0.0404	1.017
650.....	3.41	0.0701	0.0333	0.0368	1.016
700.....	3.47	0.0651	0.0313	0.0338	1.016
750.....	3.53	0.0607	0.0295	0.0313	1.016
800.....	3.58	0.0569	0.0279	0.0291	1.016
850.....	3.64	0.0536	0.0264	0.0272	1.015

[a] Parameters of molecular ion He_2^+ needed for the $S^{(ab)}(\lambda)$ and $K^{(ab)}(\lambda)$ calculations, within the 150 nm $\leq \lambda \leq$ 850 nm range.

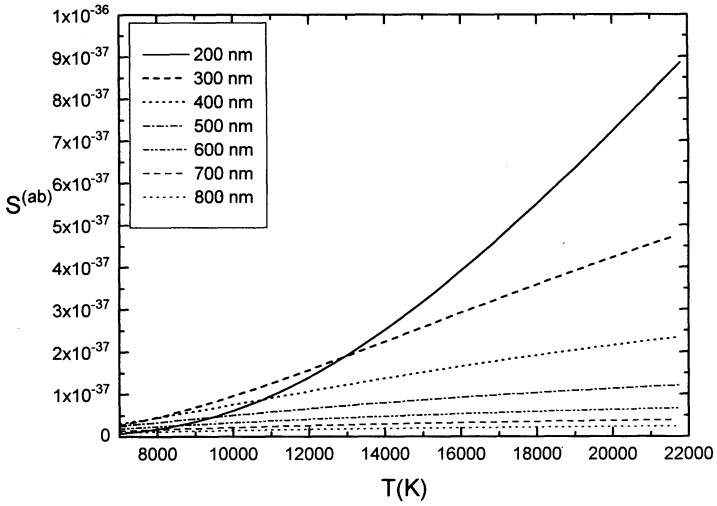

FIG. 1.—Spectral coefficients $S^{(ab)}(\lambda, T)$ for spontaneous emission resulting from ion-atom radiative processes in eqs. (1a)–(1b) together, as a function of T, for 200 nm $\leq \lambda \leq$ 800 nm.

second channel (the absorption during free-free ion-atom transitions) has been treated in a similar semiclassical way. One must recognize that both channels are, in fact, of equal importance. Moreover, for transitions in the photodissociation channel with initial rotational-vibrational states near the dissociation limit and wider (within the domain of the pronounced aharmonism), the semiclassical approach is applicable. Such a situation applies to the infrared and visible range as well. One advantage of the semiclassical approach is the simplicity of the corresponding expressions which may be easily implemented in computer codes for stellar atmosphere modeling. Moreover, eventual molecular term corrections within the presented semiclassical method need only a correction of input data given in Table 1, while in order to recalculate the quantum-mechanical results, first of all one must determine from the beginning the vibrational-rotational spectrum.

2.3. *Relative Intensities of Ion-Atom Radiative Processes*

Particular relative contributions of the ion-atom radiative processes in equations (1a) and (1b) can be characterized with the help of coefficients $X^{(a)}$ and $X^{(b)}$:

$$X^{(a,b)} = \frac{\epsilon^{(a,b)}}{\epsilon^{(ab)}} = \frac{\kappa^{(a,b)}}{\kappa^{(ab)}} . \tag{10}$$

According to Mihajlov & Dimitrijević (1992), we have that $X^{(a)} = 1 - X^{(b)}$ and

$$X^{(b)}(Z) = \begin{cases} 1 & \text{for } Z \leq 0 , \\ \Gamma(3/2;\, Z)/\Gamma(3/2) & \text{for } Z \geq 0 , \end{cases} \tag{11}$$

where $\Gamma(3/2;\, Z)$ is an incomplete gamma-function (Abramowitz & Stegun 1972) and $Z = -U_1(R_\lambda)/kT$. In considered wavelength range, we find that $U_1(R_\lambda) < 0$ and $Z = |U_1(R_\lambda)|/kT$. Here we use just the coefficient $X^{(b)}$. The behavior of this coefficient as a function of Z was shown in Mihajlov et al. (1994b).

3. RESULTS AND DISCUSSION

Our results are presented here in order to emphasize the role of the ion-atom radiative processes in equations (1a)–(1b) a

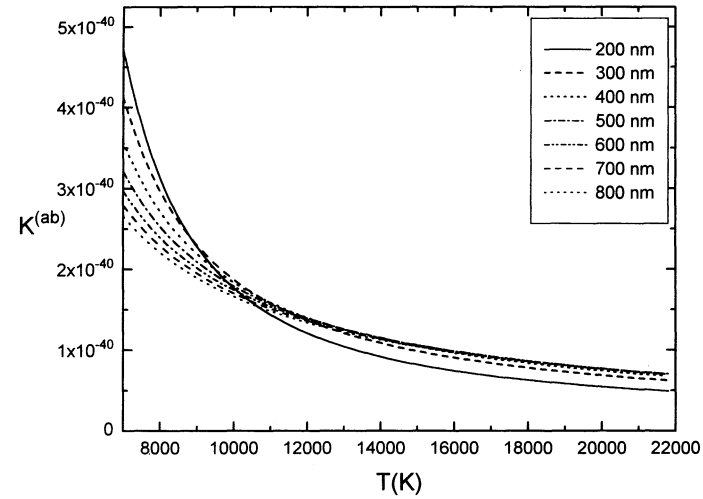

FIG. 2.—Spectral coefficients $K^{(ab)}(\lambda, T)$ for absorbtion resulting from ion-atom radiative processes in eqs. (1a)–(1b) together, as a function of T, for 200 nm $\leq \lambda \leq$ 800 nm.

source of the continuous spectrum of the DB white dwarf photospheres. The contribution of the ion-atom radiative processes in equations (1a)–(1b) is compared with the contribution of the electron-atom and electron-ion radiative processes. However, we do not consider here molecular bands generated by helium molecules in excited electronic states, or continuous spectra originating from blended lines. Present calculations for F given by equations (2) and (3) (performed by using the DB white dwarf atmospheric structures of Koester 1980) are presented in Figures 3*a*–3*e* for $\log g = 8$ and $\lambda = 200$, 300, 400, 600, and 800 nm, and in Figure 4 for $\log g = 7$ and $\lambda = 400$ nm (we note here that the figures are not on the same scale). These figures show the behavior of F as a function of the Rosseland optical depth τ (taken from Koester 1980) for $\tau \leq 2.75$. The curves in these figures correspond to the effective temperatures from 12,000 K $\leq T_{\rm eff} \leq$ 30,000 K.

In equation (2) the emissivity $\epsilon = \epsilon_{ea} + \epsilon_{ei}$. The term ϵ_{ea} is the emissivity which is due to free-free radiative transition at e-He scattering only. We take into account here the considered-atmosphere composition, in which the He component is 5 orders of magnitude larger than other components (Bues 1970; Koester 1980). We also consider the fact that the ion-atom radiative processes in equations (1a)–(1b) are significant for helium plasma with ionization degree less than or on the order of 10^{-3} (Mihajlov et al. 1993, 1994a), which also follows from our results. As a result it is quite sufficiently to take into account only e-He, among all electron-atom radiative processes. The nonexistence of the stable negative helium atomic ion, and consequently the absence of the electron photocapture during the e-He scattering, are also taken into account. The term ϵ_{ei} is the emissivity which is due to free-free (bremsstrahlung) and free-bound (photorecombination) radiative transition at e-A^+ scattering. Here A^+ denotes He^+ as well as H^+ and metal ions. We consider H^+ and metal ions have, since in a number of cases they are the significant part of the ionic component within the particular atmospheric layers; this confirms our results, which are based on Koester's (1980) data.

The term ϵ_{ea} is proportional to $N(e)$, and the term ϵ_{ei} is proportional to $N(e)^2$, where $N(e)$ is the free electron density. Consequently, the relative importance of ϵ_{ei} increases rapidly with the ionization degree; i.e., the temperature increases. Therefore, from the quick increase of just the term ϵ_{ei} follows the quick decrease of $F(\log \tau)$ in Figures 3*a*–3*e* and 4 as $T_{\rm eff}$ increases within the $T_{\rm eff} \geq$ 18,000 K range for the UV part of the spectrum and within the $T_{\rm eff} \geq$ 20,000 K range for the visible part of the spectrum. For 16,000 K for the UV range and 18,000 K for the visible range, electron-ion and electron-atom process contributions become comparable. The electron-ion term ϵ_{ei} is also responsible for the decrease of all $F(\log \tau)$ curves in these figures, for τ larger than or on the order of magnitude 1, where the temperature and the ionization degree increase quickly with the increase in τ.

When τ is less than or close to 1 and $T_{\rm eff}$ is less than or close to 16,000 K, the term ϵ_{ea} dominates in comparison to ϵ_{ei}. Consequently, within this region we find that $F(\log \tau) \approx \epsilon^{(\rm ab)}/\epsilon_{ea}$, where ϵ_{ea} may be taken as $\epsilon_{ea} = S^{\rm ff}_{ea}\, N(e)N({\rm He})$, and "ff" indicates that only the free-free electron-atom radiative processes are considered. The corresponding spectral coefficient $S^{\rm ff}_{ea}$ is taken here (as a function of λ and T) from Bell et al. (1982). It follows that

$$F(\log \tau) \approx \frac{\epsilon^{(\rm ab)}}{\epsilon_{(ea)}} = \frac{S^{(\rm ab)}}{S^{\rm ff}_{ea}} \frac{N({\rm He}^+)}{N(e)} .$$

The first multiplicator $S^{(\rm ab)}/S^{\rm ff}_{ea}$ in the above expression changes slowly (is practically constant) within the $\log \tau \leq -1$ range, but its decrease within the $\log \tau > -1$ range produces the beginning of the decrease of all $F(\log \tau)$ curves, around $\log \tau = 0$.

Figures 3*a*–3*e* illustrate the very significant influence of $T_{\rm eff}$ on the $F(\log \tau)$ curve shapes within the $\log \tau < -1$ range and for $T_{\rm eff} <$ 18,000 K. This influence is particularly pronounced for the transition from the range of $T_{\rm eff} \geq$ 14,000 K to $T_{\rm eff} =$ 12,000 K. This fact is the consequence of the behavior of the second multiplicator $N({\rm He}^+)/N(e)$ as a function of $\log \tau$ for different values of $T_{\rm eff}$. The ratio $N({\rm He}^+)/N(e)$ represents one significant characteristic of the considered plasma, namely, the relative contribution of the He atom component to the total free electron density. The behavior of this ratio as a $\log \tau$ function for $T_{\rm eff} =$ 12,000, 14,000, 16,000, and 18,000 K is shown in Figure 5*a*. One can see that within the small τ range, the He component contribution is dominant for $T_{\rm eff} \geq$ 16,000 K, is still significant for 14,000 K, and decreases sharply for $T_{\rm eff} =$ 12,000 K. Namely, at the transition between $T_{\rm eff} =$ 14,000 K and 12,000 K, the $N({\rm He}^+)/N(e)$ ratio decreases quickly for $\log \tau \leq -1$, and for $\log \tau < -1.5$, this ratio decreases for several orders of magnitude, starting from values close to 0.5 up to values close to zero (with the minimum of this ratio around $\log \tau = -3$). This follows from the Saha equation with T, $N(e)$, and $N({\rm He})$ from Koester (1980). One must take into account for the interpretation in Figure 5*a* that, for $T_{\rm eff} =$ 12,000 K and 14,000 K and $\log \tau < -1.5$, the ionization degree of the considered atmospheric layers is of the order of magnitude of 10^{-5}, and the relative contribution of the H and metals in comparison with He is 2.5×10^{-5} (Bues 1970; Koester 1980), i.e., of the same order of magnitude as the ionization degree. Accordingly, the lower curve in Figure 5*a* shows that within the $\log \tau \leq 1.5$ region, we see that an ionic component completely dominates H and metal ions for $T_{\rm eff} =$ 12,000 K, and for $T_{\rm eff} =$ 14,000 K, the contribution of the He ions becomes equal to the H and metal ion contribution. Two upper curves in Figure 5*a* illustrate the $N({\rm He}^+)/N(e)$ ratio for a further increase in $T_{\rm eff}$ from 18,000 to 20,000 K. One can see that the curve corresponding to $T_{\rm eff} =$ 18,000 K has parts in which the calculated values of this ratio are equal to 1. These parts correspond to the τ ranges for which one obtains from Koester's (1980) data that $N({\rm He}^+)/N(e) > 1$. We assumed here that $N(e) = N({\rm He}^+) + N({\rm H}^+) + N(\text{metal ions})$, where the second and third terms are the densities of H^+ and metal ions. In such cases, we assumed that $N({\rm He}^+)/N(e) = 1$ and consequently, $N({\rm H}^+) + N(\text{metal ions}) = 0$.

Within the visible part of the spectrum, the increase in the $N({\rm He}^+)/N(e)$ ratio for the transition from 14,000 to 16,000 K produces the increase in the $F(\log \tau)$ value in Figures 3*c*–3*e*. Within the UV part of the spectrum, there is no such correlation resulting from the contribution of the electron-ion radiative processes. Moreover, the contribution of these processes stops the further $F(\log \tau)$ increase with the $T_{\rm eff}$ increase over 16,000 K, within the considered spectral range.

The $F(\log \tau)$ curve oscillations in Figures 3*a*–3*e* and 4 are produced by the nonmonotonical behavior of the temperature and the electron, atom, and ion densities (as well as some of their combinations) as functions of $\log \tau$ in (or calculated from) the Koester (1980) models, which are not easy to notice at first sight. Therefore, Figure 5*b* shows the origin of such oscillations for the example of a well-pronounced oscillation within the $-5.2 \leq \log \tau \leq -4.4$ range, for $\log g = 8$ and $T_{\rm eff} =$ 14,000 K. It is taken into account that these oscillations are the most

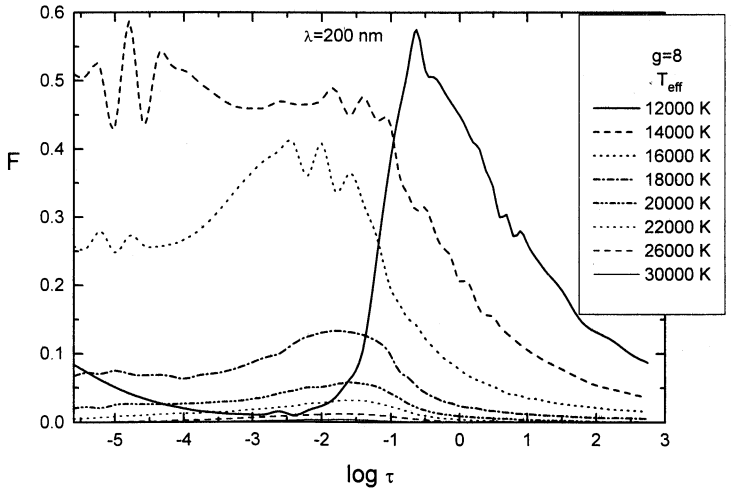

FIG. 3*a*

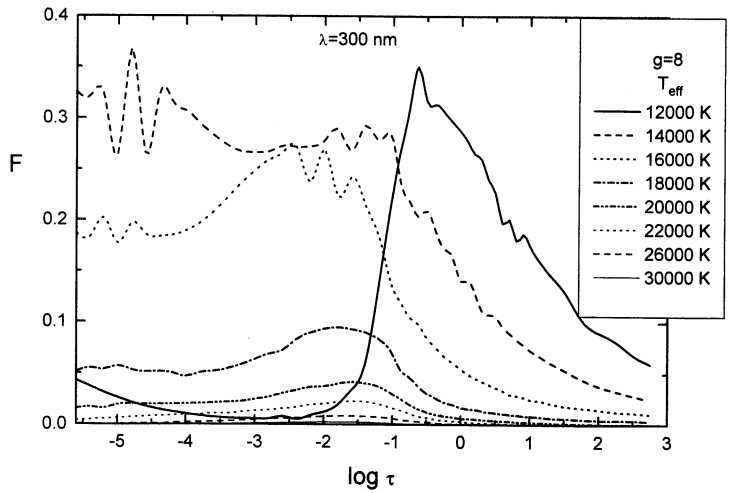

FIG. 3*b*

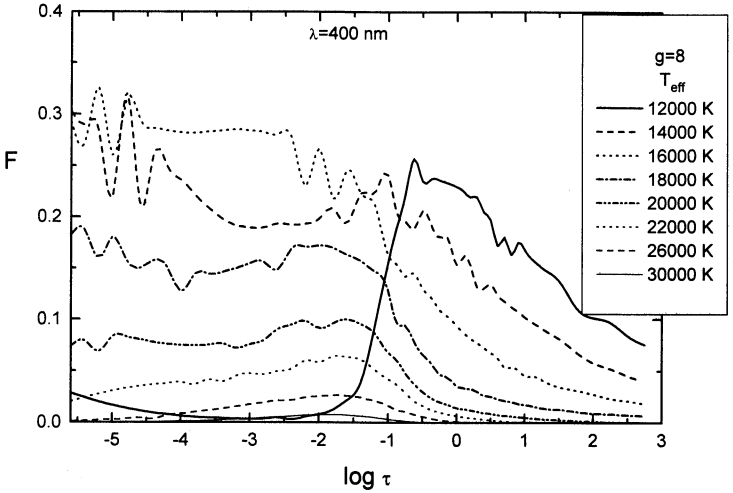

FIG. 3*c*

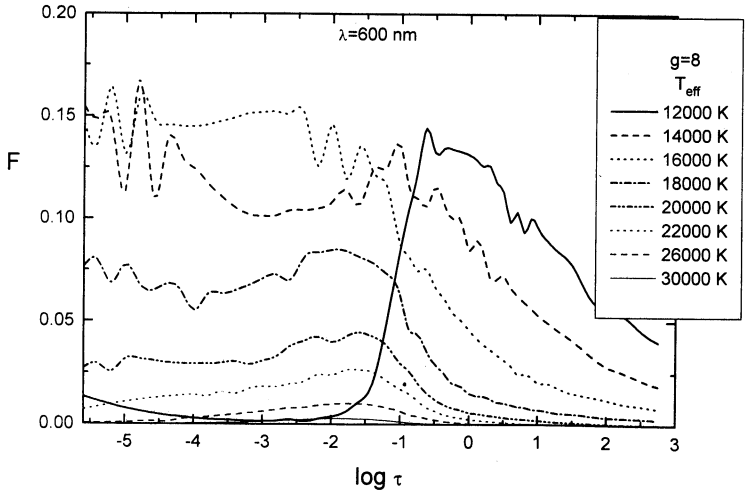

FIG. 3*d*

FIG. 3.—(*a*) Behavior of the parameter $F(\lambda, T)$, defined by eq. (2), as a function of Rosseland optical depth logarithm for $\lambda = 200$ nm and 12,000 K $\leq T_{\rm eff} \leq$ 30,000 K, in the case of $\log g = 8$. (*b*) Same as (*a*), but for $\lambda = 300$ nm. (*c*) Same as (*a*), but for $\lambda = 400$ nm. (*d*) Same as (*a*), but for $\lambda = 600$ nm. (*e*) Same as (*a*), but for $\lambda = 800$ nm.

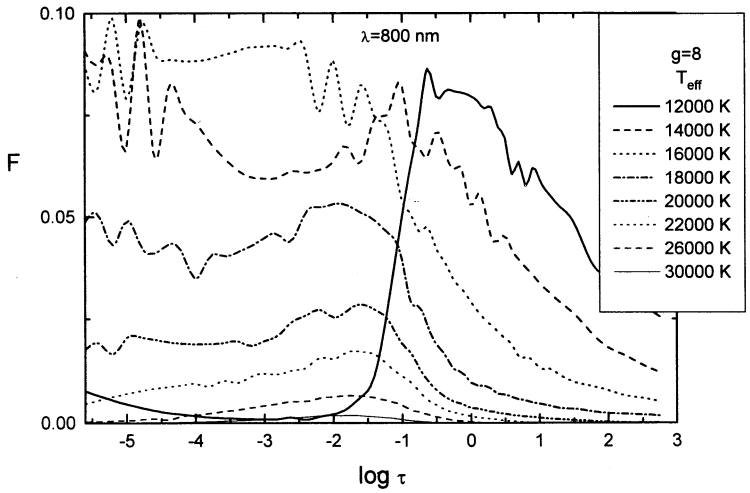

FIG. 3*e*

pronounced for $T_{eff} = 14{,}000$ K. For such well-pronounced oscillations, it is found that they are very well correlated with the corresponding oscillations of the $N(He^+)/N(e)$ ratio, which follows from the comparison of Figures 3*a*–3*e* with Figure 5*a*. In order to show the origin of oscillations, we will assume that

$$\frac{N(He^+)}{N(e)} = f_{S;He}(T)N(e)^{-2}N(He)\,,$$

where $f_{S;He}(T)$ is the Saha function of the helium component. Figure 5*b* shows the behavior of $f_{S;He}(T)$, $f_{S;He}(T)N(e)^{-2}$, and the $N(He^+)/N(e)$ ratio around the considered oscillation. In the same figure, the behavior of temperature within the considered range is shown as well. In order to present all curves in the same figure, the corresponding quantities are normalized on their values at the point $\log\tau = -4.4$. The temperature curve in Figure 5*b* illustrates that the relative temperature changes around the oscillation are very small and it is difficult to notice them. So we will show here, on the basis of Koester's (1980) data, that for $\log\tau = -5.4$, -5.2, -5.0, -4.8, -4.6, and -4.4, the temperature has the values $T = 9540$, 9612, 9601, 9740, 9703, and 9806 K, respectively. These small temperature variations, however, produce the considerable changes of the Saha function $f_{S;He}(T)$ initializating the oscillation, as shown by the lowest curve in Figure 5*b*. Such changes are the direct consequence of the large ionization potential of the He atom, but these changes are not the only reason for oscillations. The upper curve in Figure 5*b*, which shows the behavior of the product $f_{S;He}(T)N(e)^{-2}$, illustrates the large influence of the electron density variations. Finally, one can see that only when the helium atom density variations are taken into account does one obtain the real oscillation shape on the $N(He^+)/N(e)$ ratio curve. Such oscillations are not important here, however, since they are variations of several percent in relation to the general trend, which we report on here.

The change in $\log g$ from 8 to 7, however, has a considerably weaker influence on the change in the $F(\log\tau)$ curves. This may be seen by comparing Figures 3*c* and 4 for $\lambda = 400$ nm. Figures 3*a*–3*e* also show that in comparison with the electron-atom and electron-ion radiative processes, the relative influence of ion-atom radiative processes increases quickly with the λ decrease and becomes particularly significant in the UV spectral range.

In Figure 6, the relative contribution of the purely collisional

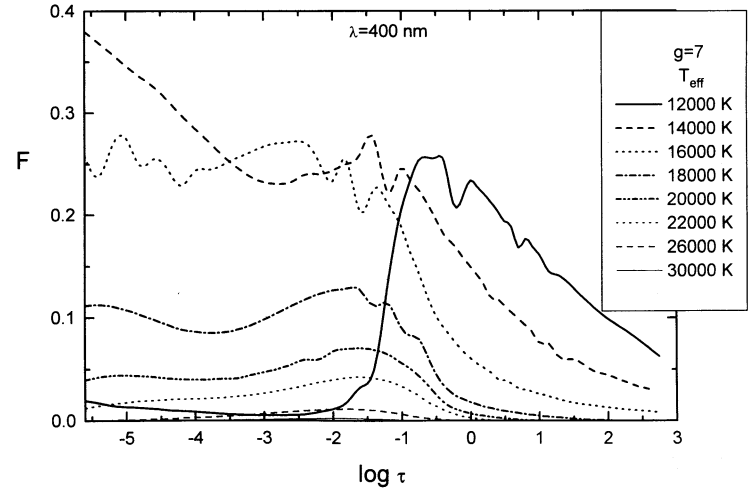

FIG. 4.—Same as Fig. 3*c*, but in the case of $\log g = 7$

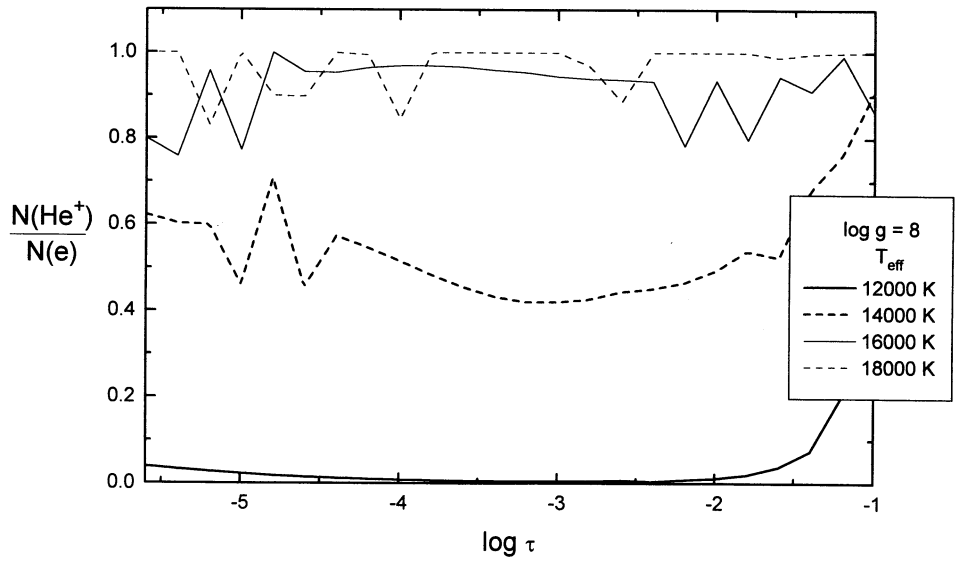

FIG. 5a

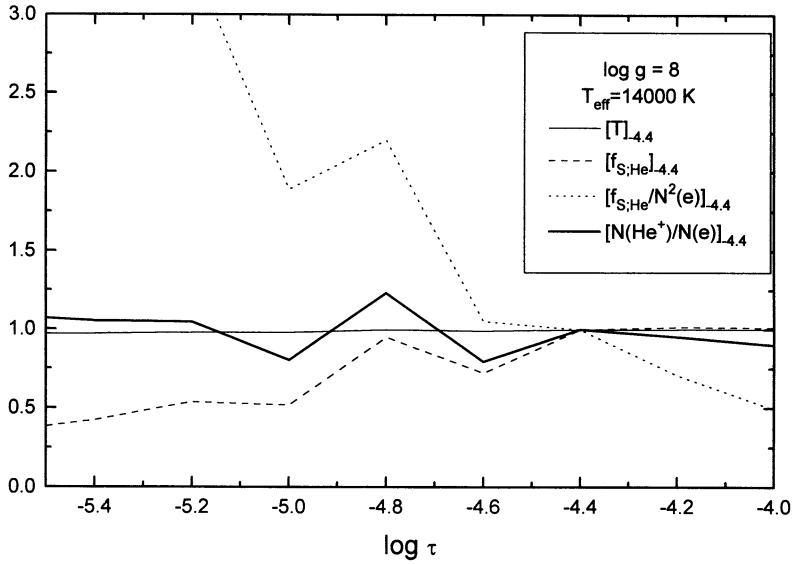

FIG. 5b

FIG. 5.—(*a*) Behavior of the $N(He^+)/N(e)$ ratio as functions of Rosseland optical depths logarithm, based on DB white dwarf models from Koester (1980). Dependence on T_{eff} for 12,000 K $\leq T_{eff} \leq$ 18,000 K and $\log g = 8$. (*b*) Behavior of the $N(He^+)/N(e)$ ratio as functions of Rosseland optical depth logarithm, based on DB white dwarf models from Koester (1980). The origin of the oscillation of this ratio for $T_{eff} = 14{,}000$ K and $\log g = 8$. Subscript "-4.4" denotes that the corresponding quantity is normalized with its value for $\log \tau = -4.4$; $f_{S;He}$ the Saha function for the He component.

radiative charge exchange processes (eq. [16]), compared to the total contribution of the ion-atom radiative processes (eqs. [1a]–[1b]), is shown. This figure is for $\lambda = 400$ nm, and one can see that the coefficient $X^{(b)}$ is weakly dependent on $\log g$. The dependence on T_{eff} is pronounced in this case as well, but the shape of the $X^{(b)}$ variation with T_{eff} remains more or less the same in the T_{eff} range considered. One can see that $X^{(b)}$ increases quickly and becomes larger than 50% around $\log \tau = 0$, so that for $\log \tau \geq 0$ the purely collisional radiative exchange processes in equation (1b) become dominant.

The influence of the ion-atom radiative processes in equations (1a)–(1b) on the optical characteristics of the considered atmospheric layers will be illustrated here with the relative changes of the optical depth and the emergent radiation intensity calculated for radial rays (see, e.g., Mihalas 1978), i.e., the ratios $\Delta\Phi(\lambda, \log \tau)/\Phi(\lambda, \log \tau)$, $\Delta\tau(\lambda, \log \tau)/\tau$, where $\Delta\Phi(\lambda, \log \tau) = [\Phi'(\lambda, \log \tau) - \Phi(\lambda, \log \tau)]$, and $\Delta\tau(\lambda, \log \tau) = [\tau'(\lambda, \log \tau) - \tau]$. Here $\Phi'(\lambda, \log \tau)$ and $\Phi(\lambda, \log \tau)$ are emergent radiation intensities determined with and without ion-atom radiative processes (eqs. [1a]–[1b]), and $\tau'(\lambda, \log \tau)$ is the optical depth determined with the ion-atom radiative processes included. In Figures 7–8 the behavior of the ratios $\Delta\tau(\lambda, \log \tau)/\tau$ and $\Delta\Phi(\lambda, \log \tau)/\Phi(\lambda, \log \tau)$ as a function of $\log \tau$, for $\lambda = 200$, 400, and 600 nm, is demonstrated. Curves in these figures are for $T_{eff} = 12{,}000$ and 14,000 K and $\log g = 8$. These curves show qualitative changes of curve shapes similar to the corresponding changes in Figures 3–4, at the transition from $T_{eff} = 12{,}000$ K to $T_{eff} = 14{,}000$ K. Moreover, similarly to Figures

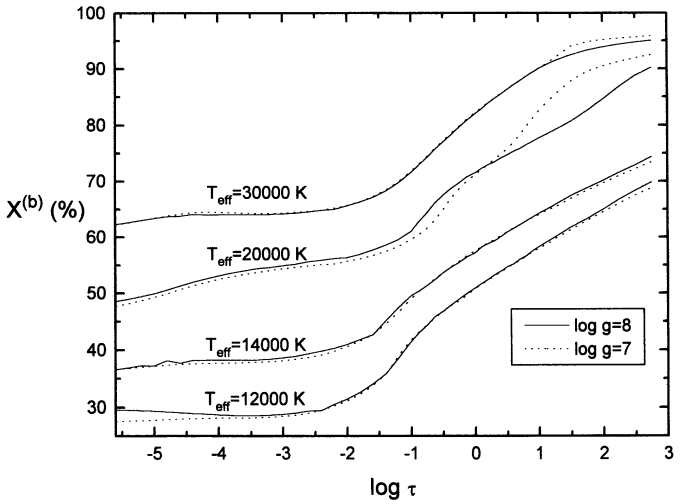

FIG. 6.—Behavior of the parameter $X^{(b)}(Z)$, where $Z = |U_1(R_\lambda)|/kT$, defined by eqs. (10)–(11), as a function of the Rosseland optical depth logarithm for $\lambda = 400$ nm, 12,000 $K \leq T_{eff} \leq 30{,}000$ K, and $\log g = 7$ and 8.

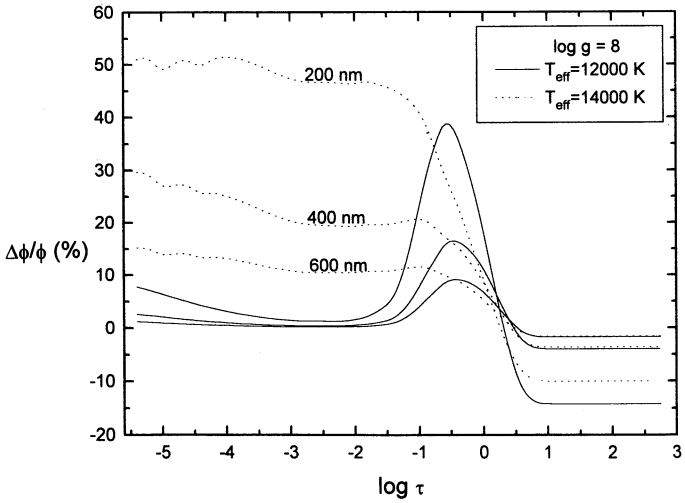

FIG. 8.—Behavior of the ratio $\Delta\Phi/\Phi$ as a function of the Rosseland optical depth logarithm for the same λ, T_{eff}, and $\log g$ as in Fig. 8.

3–4, they show the quick increase of the influence of the ion-atom processes with the λ decrease, especially at the transition from the visible to the UV spectral range. Our calculations also show that the transition from $\log g = 8$ to $\log g = 7$ is not connected with considerable changes of $\Delta\tau/\tau$ and $\Delta\Phi/\Phi$. It has been found that these changes are not larger than several percent in the largest part of the considered τ range (only for particular layers do these changes approach 20%).

The influence of the considered ion-atom radiative processes of equations (1a, b) on the optical characteristics of the atmosphere as a whole might be illustrated by the quantity $(\Delta\Phi/\Phi)_0$, i.e., by the ratio $\Delta\Phi/\Phi$, determined for $\log\tau = 0$, characterizing the whole outer layer with the optical depth $\tau = 1$. Namely, we found numerically that the further increase of the layer depth does not change the $\Delta\Phi/\Phi$ value, which is also in Figure 8. The behavior of the quantity $(\Delta\Phi/\Phi)_0$ is shown in Figure 9 as a function of λ within the 200 nm $\leq \lambda \leq$ 800 nm range, for 12,000 K $\leq T_{eff} \leq$ 20,000 K and $\log g = 8$. One can see that the relative intensity change is negative and decreases by up to 14%. We note that the final $(\Delta\Phi/\Phi)_0$ values characterize at the same time the influence of the absorption channel which decreases this value and the emission channel which leads to its increase. For the considered case, we find that in the contribution of the ion-atom radiative processes of equations (1a)–(1b) the influence of the absorption channels dominates. We found here that the final $(\Delta\Phi/\Phi)_0$ values are not negligible. Moreover, Figure 7 shows that changes in the optical depth $\Delta\tau$ represent a significant disturbance of the reference value τ for the tabular presentation of the white dwarf model, rather than a small perturbation. One can see in Figure 8 as well that $\Delta\Phi$ is a strong perturbation for energetic balance considerations of particular atmospheric layers. Consequently, the ion-atom radiative processes in equations (1a)–(1b) must be taken into account during the white dwarf atmosphere modeling and not added a posteriori as a correction to the result obtained by using the model when such processes have been neglected.

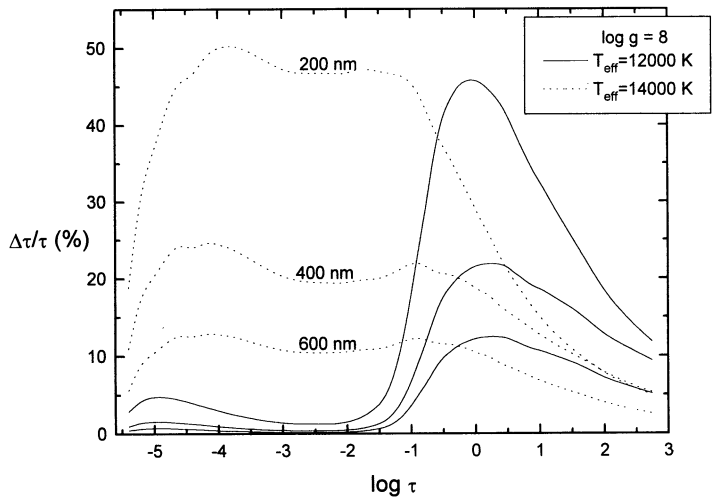

FIG. 7.—Behavior of the ratio $\Delta\tau/\tau$ as a function of the Rosseland optical depth logarithm for $\lambda = 200$, 400, and 600 nm and $T_{eff} = 12{,}000$ and 14,000 K, in the case of $\log g = 8$.

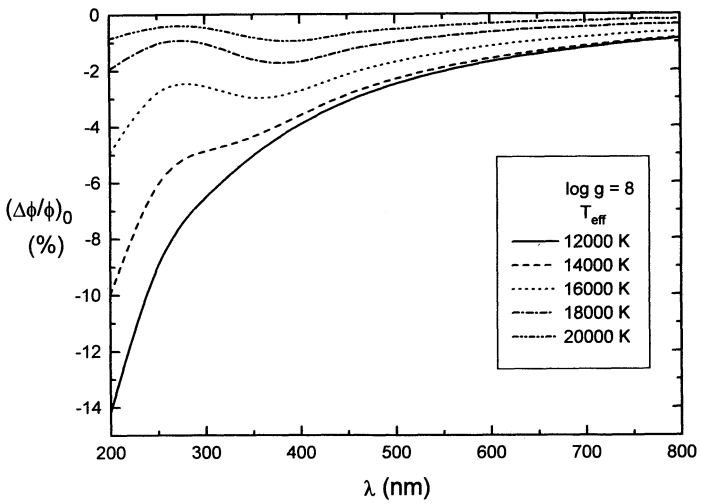

FIG. 9.—Behavior of the quantity $(\Delta\Phi/\Phi)_0$, i.e., the ratio of $\Delta\Phi/\Phi$ as a function of λ for T_{eff} and $\log g$ as in Fig. 6. Here $(\Delta\Phi/\Phi)_0$ denotes the ratio of $\Delta\Phi/\Phi$ for $\log\tau = 0$.

4. CONCLUSIONS

It is shown in this article that for $T_{eff} \leq 16{,}000$ K, DB white dwarf photosphere continuous spectra are formed under the important influence of the ion-atom radiative processes, while for larger T_{eff} values the electron-atom and electron-ion processes have a more basic role. This is the consequence of the fact that the influence of ion-atom radiative processes increases quickly when T_{eff} decreases around $T_{eff} = 16{,}000$ K. Moreover, a large increase in the H and metal relative contribution to the total electron density was found at the transition from $T_{eff} =$ 14,000 K to 12,000 K. This results with the very significant $He^+ + He$ relative emissivity curve shape change for $T_{eff} =$ 14,000 K and 12,000 K. It is also found that the influence of the radiative ion-atom processes increases quickly when λ decreases, especially at the transition from the visible to the UV spectral range.

From the results shown, it follows that for $T_{eff} \leq 16{,}000$ K and $\lambda \leq 400$ nm, ion-atom radiative processes may influence significantly the energetic balance and optical characteristics (opacity and optical depth) of white dwarf atmospheric layers where $\log(\tau) \leq 1$. Especially important is the influence on the optical depth values calculated with and without taking into account the ion-atom radiative processes. The facts presented suggest that it is necessary to include ion-atom radiative processes for the white dwarf atmosphere modeling from the beginning and not as an a posteriori correction, since they change the reference optical depths for the tabulated model parameters. All elements needed for the inclusion of the ion-atom radiative processes in the DB white dwarf atmosphere modeling are presented here.

REFERENCES

Abramowitz, M., & Stegun, I. 1972, Handbook of Mathematical Functions (New York: Dover)
Bell, K. L., Berrington, K. A., & Croskery, J. P. 1982, J. Phys. B, 15, 977
Bues, I. 1970, A&A, 7, 91
Ermolaev, A. M., & Mihajlov, A. A. 1991, J. Phys. B, 24, 155
Gupta, B. K., & Madsen, F. A. 1967, J. Chem. Phys., 47, 48
Koester, D. 1980, A&AS, 39, 401
Menzel, D. H. 1962, Selected Papers on Physical Processes in Ionized Plasmas (New York: Dover)
Mihajlov, A. A., & Dimitrijević, M. S. 1986, A&A, 155, 319
———. 1992, A&A, 256, 305
Mihajlov, A. A., Dimitrijević, M. S., & Ignjatović, Lj. 1994a, A&A, 287, 1026
Mihajlov, A. A., Dimitrijević, M. S., Ignjatović, Lj., & Djurić, Z. 1994b, A&AS, 103, 57
Mihajlov, A. A., Ermolaev, A. M., & Dimitrijević, M. S. 1993, J.Q.S.R.T., 50, 227
Mihajlov, A. A., & Popović, M. M. 1981, Phys. Rev. A, 23, 1679
Mihalas, D. 1978, Stellar Atmospheres (San Francisco: W. H. Freeman)
Sobelman, I. I. 1979, Atomic Spectra and Radiative Transitions (Berlin: Springer-Verlag)
Stancil, P. C. 1994, ApJ, 430, 360
Vernazza, J. E., Avrett, E. H., & Loeser, R. 1981, ApJS, 45, 635